Supercavitating Object Propulsion

Yu. N. Savchenko
Ukrainian National Academy of Sciences - Institute of Hydromechanics
8/4 Zhelyabov str., 03057 Kiev
Ukraine

1. SC vehicle as a result of tendencies of high speed vehicle development

In practice, the vehicle development is stipulated by a useful effect that is attained upon the vehicle operation.

The useful effect for transport ships consists in cargo transportation. Thus, the ship efficiency as vehicle efficiency will be determined by commercial effectiveness [22]

$$K_p = \frac{PV}{N},$$

where P is the payload, V is the velocity, N is the power.

The velocity and range are determining parameters for objects used for military and rescue purposes. In this case one can see that the hydrodynamic drag reduction positively influences on all main characteristics and increases the commercial effectiveness coefficient owing to consumed power decrease or increase of the velocity and range.

For surface vehicles, we clearly see a tendency of decreasing the waterline area and wetted surface of the hull due to dynamic means of maintenance of the hull on the water surface. There are ships with small waterline area SWATHS, hydrofoil ships, hovercrafts, ekranoplanes and hydroplanes.

In this case the energy consumption to realize the dynamic means of maintaining the hull on the water surface may be related to the controlling effect for the drag reduction.

One can see in Fig. 1 that the velocity and specific power of the vehicles increases at exiting the hull from the water.

The same way of reduction of the wetted surface of the hull due to developed artificial or vapor cavitation – supercavitation [10, 11, 15] may be used for underwater motion.

Calculations shows it is possible to obtain a twenty-fold advantage in the hydrodynamic drag when the velocity is equal to 100 m/sec, and cavitation number σ = 0.01, and 1000-fold advantage may be obtained when the cavitation number $\sigma = 10^{-4}$ [11].

$$\sigma = \frac{p_0 - p_c}{\rho V^2 / 2},$$

where p_0 is the hydrostatic pressure, p_c is the cavity pressure, which is equal to the saturated water vapor pressure $p_c = p_v$ at vapor cavitation.

Paper presented at the RTO AVT Lecture Series on "Supercavitating Flows", held at the von Kármán Institute (VKI) in Brussels, Belgium, 12-16 February 2001, and published in RTO EN-010.

Comparing the efficiency of the different methods of the hydrodynamic drag reduction with efficiency of the artificial and vapor supercavitation, one can see its advantage and, hence, perspective of its use [22]. Moreover, a vapor layer between the water and hull unites many methods of the drag reduction:

- Reduction of water adhesion to the surface or slippage;
- Effect of the movable surface (the gas flow velocity in the clearance may be equal to the water flow velocity);
- Change of the physical constants of BL (here, the medium density reduction);
- Gas blowing into the boundary layer (BL).

Here, – in the case of the artificial cavitation, the gas is blown through the solid surface of the object.

– in the case of vapor supercavitation, the gas arrives from the supercavity surface.

However, use of the supercavitation flow schemes requires respectively high specific power of the vehicle. So, when the velocity is equal to 100 m/sec, and cavitation numbers $\sigma = 0.05 \div 0.01$, specific available power will be of order $\frac{N}{D} = 2000 \div 4000$ H.p./t This is compared with specific power of the planing ships in the universal diagram of Gabrielly-Karman [22] (Fig. 2) .

2. Features of supercavitation

First of all, the supercavitation flow regime gives limitations for shape and dimensions of the hull of an underwater vehicle. They must correspond to the calculated supercavity shape. Therefore, formalization of the hull geometry will be performed by comparing the vehicle volume and surface with the supercavity volume and surface or with shapes of hulls of Reichhardt series having the constant pressure [19].

In this case dimensions of the vehicle having a shape of a body of revolution will be restricted by limiting dimensions of the supercavity. They are determined by known formulae for main supercavity dimensions [1]

$$D_c = D_n\sqrt{\frac{c_x}{\sigma}}; \qquad L_c = \frac{D_n}{\sigma}\sqrt{c_x \ln\frac{1}{\sigma}}; \qquad \lambda = \frac{L_c}{D_c} = \sqrt{\frac{\ln\frac{1}{\sigma}}{\sigma}}, \tag{1}$$

where cavitation number $\sigma = 2(p_0 - p_c)/\rho V^2$ is a main parameter of the supercavitation flows, p_0, p_c are pressures in the stream and in the cavity, respectively, and $c_x = c_{x0}(1+\sigma)$ is the coefficient of this cavitator in the form of a disk with diameter D_n, c_{x0} is the drag coefficient when $\sigma = 0$.

We should note that the supercavitation motion regime requires enough high motion velocity that is sufficient to form a supercavity where the vehicle hull is inscribed completely. This is explained by structure of the formulae for main supercavity dimensions (1):

$$\frac{D_c}{D_n} = V\sqrt{\frac{\rho c_x}{p_0 - p_c}}; \qquad \frac{L_c}{D_n} = \frac{\rho V^2}{p_0 - p_c}\sqrt{c_x \ln\frac{1}{\sigma}}. \tag{2}$$

The object calculated for given regime and inscribed into the calculated supercavity will need the attainment of this calculated velocity in the unseparated flow regime. During acceleration some difficult problems arise. These are:

– energetic problem connected with overcoming

the high hydrodynamic drag of the vehicle in unseparated flow;

– problem on ensuring the motion stability in

non-calculated flow regime.

The second essential feature of the supercavitation motion is a necessity to take into account the energy expenditure, volume and mass to ensure artificial regime of supercavitation, i.e. gas blowing into the cavity. This is inevitable upon the object acceleration up to the calculated velocity and maintaining the supercavity in sub-vapor supercavitation regimes when the pressure in the cavity is higher that the pressure of saturated water vapors. The necessity of the gas-supply into the cavity disappears at attainment of vapor supercavitation regimes when the supercavity is filled by water vapor.

The problem of interaction between the propeller and supercavity is sensitive to the velocity and pressure perturbations caused by working propeller. This may result in additional washing the hull and increasing the gas-supply rate.

In the general case the supercavitating vehicle motion may be considered as one consisting of three phases :

– phase 1 – the vehicle acceleration up to the calculated velocity;

– phase 2 – motion with constant velocity;

– phase 3 – motion on inertia.

The known applications of the supercavitation motion are used to attain the maximal motion range in phase 2 or in phase 3. In this case phase 1 is not essential to pass the distance, but has decisive significance in the propulsive sense, since requires development of the highest power exceeding multiply the power necessary for motion with constant calculated velocity.

3. Energy of SC vehicles in stationary motion

Energy of SC vehicles in the stationary motion will be determined by their hydrodynamic drag in steady flow. Since the vehicle hull will place in a vapor or gas cavity, the main component of the hydrodynamic drag is the cavitator drag. It is determined by formula

$$R_x = \frac{\rho V^2}{2} c_x S_n, \tag{3}$$

where ρ is the fluid density, V is the motion velocity, c_x is the cavitator drag coefficient (for disk $c_x = 0.82(1+\sigma)$, where σ is the cavitation number), $S_n = \frac{\pi D_n^2}{4}$ is the cavitator area.

Additional hydrodynamic drags can arise owing to using the schemes of supercavitation flow with partial or periodic washing the tail part of the object. Fig. 3 shows possible schemes of supercavitation flow around SCO:

a) scheme of flow with forming two cavities;

b) stationary planing along the inner cavity surface;

c) periodic impact interaction with the cavity walls;

d) aerodynamic interaction with vapor-splash medium of the cavity.

In the general case the total hydrodynamic drag of SCO may be represented with taking account of the cavitator drag (3) in the form

$$R_x = R_{xn} + R_{xF}, \tag{4}$$

where R_{xF} is the additional hydrodynamic drag of friction upon washing the hull. It may be equal $R_{xn} \cong 0.01 R_{xn}$ at the flow scheme d) (Fig. 3) and $R_{xn} \cong 0.5 R_{xn}$ at the flow scheme a) (Fig. 3).

When $V = Const$, the propeller thrust T must equalize the drag (4)

$$T = R_x. \tag{5}$$

If the propeller is one of rocket type, its thrust will be equal

$$T = \dot{m}_f Q_f, \tag{6}$$

where $\dot{m}_f = dm/dt$ is the mass rate of the fuel, Q_f is the specific impulse of the fuel.

For steady motion when $\dot{m}_f = Const$,

$$T = \frac{m_f}{t} Q_f. \tag{7}$$

Using the formulae (3) – (7), we obtain

$$V = \sqrt{\frac{2}{c_x \rho S_n}} \cdot \sqrt{\frac{m_f}{t} Q_f}. \tag{8}$$

Introducing the passed distance S in the form

$$S = Vt. \tag{9}$$

and define the volume due to the fuel

$$W_f = m_f / \rho_f = const, \tag{10}$$

we obtain for the passed distance that

$$S = \sqrt{\frac{2W_f}{c_x \rho S_n}} \cdot \sqrt{\rho_f Q_f t} = C_1 \sqrt{\rho_f Q_f t}\,, \tag{11}$$

where $\sqrt{\frac{2W_f}{c_x \rho S_n}} = C_1 = Const$, ρ_f is the fuel density.

One can see in the expression (11) that to attain the maximal range S it is necessary to apply fuels with maximal specific impulse Q_f and density ρ_f.

The vehicle velocity is obtained from expressions (3) and (5)

$$V = \sqrt{\frac{2}{c_x \rho}\left(\frac{T}{S_n}\right)}. \tag{12}$$

We can see from here that the velocity is proportional to ratio $(T/S_n)^{1/2}$.

We can obtain the estimation of maximal range from the assumption that whole cavity volume is filled by the vehicle hull, and the hull is filled by fuel with density ρ_f and specific impulse Q_f.

As since the cavities have a shape close to an ellipsoid with known diameter and length (1), it is possible to calculate the supercavitry volume W_c with taking account of the relation $L_c = \lambda D_c$ (1)

$$W_c = 0.71\pi R_c^2 L_c\,. \tag{13}$$

The SCO drag will be equal [1]

$$R_x = c_x \frac{\rho V^2}{2} S_n = k S_c \Delta P\,, \tag{14}$$

where $S_c = \pi R_c^2$ is the cavity mid-section area, $\Delta P = p_0 - p_c = \sigma \frac{\rho V^2}{2}$ is the pressure difference, $k = 0.96$.

The fuel mass in the cavity volume

$$m_f = \rho_f W_c = 0.71\pi R_c^2 L_c \rho_f\,. \tag{15}$$

Time, when the propeller is maintaining the necessary thrust, or the motion time is

$$t = \frac{Q_\Sigma}{R_x}, \tag{16}$$

where $Q_\Sigma = m_f Q_f$ is the total impulse of the fuel.

Hence, the maximal range of the motion S will be equal

$$S = tV = 1.4 \frac{\rho_f}{\rho} \frac{Q_f}{V} \frac{L_c}{\sigma} \tag{17}$$

or in the dimensionless form

$$\overline{S} = \frac{S}{L_c} = 1.4 \sigma^{-1} \frac{\rho_f}{\rho} \frac{Q_f}{V}. \tag{18}$$

If we assume that metal fuel of high efficiency is used ($\rho_f / \rho = 2.7$; $Q_f / V = 30$; $\sigma = 0.01$; $L_c = 10$ m), then the maximal range will be equal to

$$\overline{S} = 1.4 \cdot 100 \cdot 30 \cdot 2.7 = 11340$$

or in dimensional form $S = 113400$ m.

When the solid rocket fuel on the basis of nitrocellulose and nitroglycerin – JPN with density $\rho_f = 1.6$; $Q_f / V = 11$ is used, then the maximal range will be equal

$$\overline{S} = 1.4 \cdot 100 \cdot 1.6 \cdot 11 = 2464,$$

$$S = \overline{S} L_c = 24640 \text{ m}.$$

Calculation of maximally attainable range is represented in graphic form in Fig. 4. Here, the range S is represented as a dependence on velocity V and aspect ratio of the hull (cavity) $\lambda = L_c / D_c$ for specific impulses of the fuels Q_f = 230 sec and Q_f = 600 sec, depth H = 10 m, L_c = 10 m. If it is assumed that the strengthening (design) restriction of the hull aspect ratio is $\lambda \le 20$, then the maximal restriction on the motion range of SCO is $S_{\max} = 70$ km and on the velocity $V_{\max} = 200$ m/sec.

3.1. UNDERWATER VEHICLE PROPELLERS

Underwater vehicle propulsion is intended to transform chemical energy of the fuel into thermal energy. The latter transforms into mechanical energy – work for overcoming the hydrodynamic drag R_x (3).

When the motion is uniform, the thrust T of the propeller must equalize the hydrodynamic drag R_x

$$T = R_x . \tag{19}$$

In this case the useful power of the underwater vehicle propulsion will be equal to

$$N = TV . \tag{20}$$

The propulsion effectiveness is estimated by its total efficiency η representing the ratio of useful power N and all consumed power

$$\eta = \frac{TV}{I\dot{q}}, \tag{21}$$

where I is the mechanical equivalent of heat; $\dot{q}$ is the heat rate per time unit.

The coefficient η characterizes the propulsion perfection and is dependent of the fuel characteristics. In practice, the specific rate of the fuel is of importance. It is quantity of the fuel consumed per time unit at unit power. It is usually measured in g/kilo-Watt·hour. Since $\dot{q} = q \cdot \dot{m}_f$, where q is the caloric ability of the fuel; $\dot{m}_f$ is the fuel rate per a second.

Using (21), we obtain the relation for the specific rate of the fuel and efficiency η

$$\dot{q}_f = \frac{\dot{m}_f}{TV} = \frac{1}{I\,q\eta} . \tag{22}$$

One can see from (22) that the specific rate of the fuel $\dot{q}_f$ depends both on the propulsion characteristics η and on the fuel characteristics q. For diesels

$\dot{q}_f$ = 215 g/kW · h, for turbines $\dot{q}_f$ = 340 g/kW · h.

We well know specific powers of different propulsions used in the underwater vehicles [4]. There are

diesel propulsions	45 ÷ 90 W/kg	10 ÷ 30 W/ m^3
electro-accumulators	60 ÷ 100 W/kg	200
atomic propulsions	25 ÷ 200 W/kg	11.3
high-speed diesels	1.33 kW/kg	224 kW/ m^3
gas turbines	5.7 kW/kg	1700 kW/ m^3

It is known as well that the turbine or piston propulsion volume does not exceed 50% of the vehicle volume, whereas the fuel part in rockets exceeds 90%.

It is essential that the necessary specific power for supercavitating vehicles is calculated by formula

$$\rho_v = \frac{R_x V}{W_c} = \frac{R_x V}{0.67\pi R_c^2 L_c} = 0.71 \frac{\sigma \rho V^3}{L_c}. \qquad (23)$$

When $\sigma = 0.01$, $L_c = 10$ m, $\rho_v = 715$ kW/m^3 at V = 100 m/sec; $\rho_v = 5720$ kW/m^3 at V = 200 m/sec.

These values exceed on 2 – 3 orders the analogous values for diesel, electric, atomic propulsions. Therefore, the gas-turbine and jet propulsions with the metal fuel and using outboard water as a oxidizer and a cooler of the combustion products are considered perspective ones for the supercavitating vehicles at increased motion velocity. Such propulsions were investigated experimentally, and their high efficiency was confirmed [19].

At that, the increase of the velocity of SCO motion compared with vehicles at unseparated flow up to 100 – 200 m/sec do attractive the rocket schemes with solid fuel in view of the propulsion efficiency increase

(Fig. 5)

$$\eta_p = \left[1 + \frac{1}{2}\left(\frac{V_j - V}{V_j}\right)\right]^{-1}. \qquad (24)$$

Fig. 5 represents a graph of dependence of the propulsive efficiency for the jet propeller with solid fuel on the motion velocity at $V_j = 2040$ m/sec.

Reaction Al + water gives high temperature 10800K. Therefore, water must be supplied into the propeller in plenty. In this case the propulsion temperature reduction will occur according to the theoretical dependence on water gram-molecules n (Fig. 6a).

It is well known that to accelerate the reaction it is necessary to fluidize the metal and to transform the water into vapor. The calculation of the thermal processes is performed at condition that the temperature of the reaction products was reduced to 1250K. A scheme of the propulsion working on fuel Al with using the outboard water is shown in Fig. 6b. In the presented propulsion, the heat from combustion chamber is transmitted to aluminum to form a melt at temperature about 950K and to water to form vapor. The combustion products arrive on the turbine and after the turbine to outboard. In this case the propulsion efficiency will depend essentially on the excess pressure in the combustion chamber on the different depths. This is shown in graph in Fig. 7.

The graph in Fig. 7 gives the dependence of the specific output power of the propulsion with the fuel – aluminum + sea-water for different depths H = 305 ÷ 1525 m. For supercavitation motion regimes, the vapor exhaust will occur into the supercavity at pressure P = 0.02 kg/cm^3. This corresponds to the saturated vapor pressure at temperature 15°C. This pressure corresponds to the air pressure on height 23 km above sea level and ensures ideal conditions for work of propulsions with opened cycle independently on the object motion depth.

A scheme of the turbo-rotor propeller for supercavitating vehicle was considered to increase its efficiency at the Institute for Fluid Mechanics. Propellers with one or two turbo-rotors (Fig. 8, a,b,c) were tested there. It is shown in the scheme that the gas turbine and screw with three blades working in supercavitation regime were combined on one disk of the rotor. There also are shown section of the turbine blades and supercavitating screw sections.

Photographs in Fig. 9 a,b,c show models of the turbo-rotors in the hydro-tunnel and a picture of flow around the working turbo-rotors in the hydro-tunnel when the free stream velocity V = 10 m/sec at using the gas turbine with compressed air and at pressure to 6 kg/cm^2.

Preliminary experiments with turbo-rotor propellers showed real possibility of the propeller thrust increase on 20 % compared to the rocket scheme, although theoretical estimations point to possibility of double increase of the thrust. Therefore, possibility of attainment of optimal conditions for work of the turbine and supercavitating screw still will have to be realized.

3.2 FUEL FOR SCO

We can see from the previous analysis that the fuel for high-speed SCO must satisfy the heightened requirements to the specific characteristics Q_f and ρ_f. The specific characteristic - power/volume is the more important than the power/mass.

Work [21] considers schemes of turbo-prop of the hydro-jet propeller working on unitary solid fuel (Fig. 10, a), on two-component fuel (Fig. 10, b) and on hydro-reacting fuel on the basis of reaction between the magnesium and sea-water (Fig. 10, c).

Calculations showed that ratios of specific rates of the fuel transported on the board $\dot{m}_{fa} = \dfrac{\dot{m}_f}{T}$ in wide velocity range 20 ÷ 100 m/sec have constant values

$$\frac{\dot{m}_{fa}(schem\ b)}{\dot{m}_{fa}(schem\ a)} = 0.42; \quad \frac{\dot{m}_{fa}(schem\ c)}{\dot{m}_{fa}(schem\ a)} = 0.37.$$

The relations show that the hydro-reacting fuel on the vehicle board must be in 1.15 times less than the two-component one (scheme b) and in 2.7 times less than the solid unitary fuel (scheme a).

In rocket systems, where the fuel mass predominates, and weight and volume of the nozzle and combustion chamber are comparatively small, the propulsive characteristics of the system will be determined by the fuel characteristics – its specific impulse Q_f and density ρ_f.

The investigations showed that the chemical fuels using metals and sea-water as oxidizer, ballast and cooler are the most effective for underwater vehicles. This is stipulated that the metals ensures maximal energy at reaction with water [19, 21]

Al + sea-water → 3143 kW·hour/m^3 (1.18 kW·hour/kg),

Mg + sea-water → 1891 kW·hour/m^3 (1.05 kW·hour/kg),

Li + sea-water → 1092 kW·hour/m^3 (2.09 kW·hour/kg).

Reactions and main parameters are presented in Table [19, 21] Fig. 11.

In practice, Al is the best fuel, since it is proof and cheap. Aluminum melting temperature is 950K, and the combustion temperature in reaction with H_2O reaches 10800K.

Perspective of the fuels for the underwater vehicles is frequently estimated by theoretical value of specific work of the jet flow (kW·h/m^3). It is determined at fixed value of the balanced expansion and quantity of the injected sea-water sufficient to decrease the combustion product temperature to 1250K.

Dependence of the approximate theoretical values of the specific power with respect to mass ρ_1 and volume ρ_2 for *Al* at reaction with water

$$2Al + n \cdot H_2 0, \tag{25}$$

where n is the number of gram-molecules upon expansion of the combustion products from 206.9 to 10.14 kN/m^2, is presented in Fig. 12.

4. Calculation of supercavitating model motion range at inertial motion

Drag of a supercavitating model completely enveloped by a cavity is equal to a cavitator drag and calculated by formula

$$R_x = \frac{\rho V^2}{2} c_{xn} S_n, \tag{26}$$

where ρ is the fluid density; V is the model velocity; c_{xn} is the cavitator drag coefficient (for disk c_{xn} = 0.82 (1 + σ), where σ is the cavitation number); S_n is the cavitator area.

When cavitation number is small, it is possible to consider c_{xn} as constant one. Then the equation of motion of the model with mass *m* has the form

$$\frac{dV}{dt} = -kV^2, \tag{27}$$

where $k = \frac{\rho c_{xn} S_n}{2m}$.

Its solution gives dependence of motion time on velocity in the form

$$t(V) = \frac{1}{k}\left(\frac{1}{V} - \frac{1}{V_0}\right) \tag{28}$$

and dependence of passed range S on the velocity in the form

$$S(V) = \frac{1}{k} \ln \frac{V_0}{V} \quad , \tag{29}$$

where V_0 is the starting velocity of the model.

Hence, the model moves infinitely long and passes infinitely great distance. It is necessary to define criterion determining the finite point of the path to have sense of the range calculation.

Such criteria can be:

– the velocity reduction to certain value;

– decrease of the model momentum to certain value;

– disappearance of clearance between the model and cavity walls.

In essence, the second and third criteria are distinctive from the first one only by way of the final velocity definition. Thus, it is possible to consider the final velocity V_e definition as the most universal way of determination of the motion range S_e.

The range depends on the model mass m and cavitator radius r_p determining the drag for given velocities V_0 and V_e.

As the model must be located in the cavity, its maximal possible mass depends on the material density ρ_b, model length L and cross cavity dimensions determined by the cavitator radius.

Thus, the range is determined by

– material density;

– model length;

– cavitator radius.

Calculations necessary to determine the range can be executed due to the program SCAV [23]. The model shape is approximated by three truncated cones (Fig. 13, a) in this program. The program computes:

– the model characteristics: volume, mass center location and moment of inertia;

– the shape and dimensions of stationary supercavity past a disk or a conic cavitator at given velocity and depth of the motion;

– the clearances between the model and cavity boundary;

– the value of impact load acting to the model at water entry;

– the speed reduction of the supercavitating model moving on inertia;

– the basic dimensions of unsteady cavity (length and mid – section diameter) in any point of the distance.

The SCAV program (SuperCavity, Version 1.3) is intended to automatize designing the high-speed supercavitating models.

At experimental investigations of high-speed motion in water, the model shape must satisfy requirements of inscribing into a natural cavity and structural stability of the supercavitating motion regime. If we suppose that the model moves rectilinearly under action the cavitation drag only, then the process is described by the dimensionless equation of model motion on inertia

$$\frac{dV}{dt} = \frac{1}{Fr^2} - \frac{\rho \pi D_n^3 c_{x0}}{8m}\left[V^2 + \overline{p}_{atm} + \frac{2H}{Fr^2} - \overline{p}_c(t)\right],$$

where m is the mass of model; c_{x0} is the cavitation drag coefficient when $\sigma = 0$, p_{atm} is the atmospheric pressure; H is the immersion depth.

Fig. 13, a presents a copy of PC-screen after calculation of the model location in the cavity. The model shape and starting data correspond to the real experiment. The vertical scale of the image is increased for clearness.

In Fig. 13, b, graphs of changing the cavity length L_c and model velocity V in dependence on passed distance x are shown. The calculation was executed for titanic model at $D_n = 1.5$ mm, m = 49.0 g, $V_0 = 1000$ m/s. It is supposed that the model enters in water in point $x = 0$ and then moves on inertia. The initial rectilinear part of the graph $L_c(x)$ corresponds to the interval of the supercavity formation. Quasistationary magnitudes of $L_c(x)$ are plotted by dashed lines for comparison.

4.1. INERTIAL MOTION WITH PROPELLER

Motion of the model with propeller has two features. First, thrust T_p acts on the model. It compensates the drag. Second, the part of the model material with density ρ_b must be changed by fuel with density in 4 times lower. Therefore, the model mass with propeller, especially in the path end, is lower than the solid model mass.

The missile thrust can be determined from the relation behavior

$$T_p = -Q_f \frac{dm_f}{dt}, \tag{30}$$

where T_p is the propeller thrust; m_f is the fuel mass; Q_f is the specific impulse of the fuel. Usually, its value is expressed in kg_f/(kg/sec) or lb_f/(lb/sec). Numerical magnitudes are equal in the both cases.

Typical magnitudes of Q_f are in range from 200 to 500 kg_f/(kg/sec). Passing onto the system SI, we obtain

$$Q_f' = 9.81 Q_f \frac{n \cdot \sec}{kg} = 9.81 Q_f \frac{kg \cdot m}{\sec^2} \frac{\sec}{kg} = 9.81 Q_f \frac{m}{\sec}.$$

Impulse of force T_p during the motion time is

$$K_f = Q_f' m_f. \tag{31}$$

If the propeller chamber volume is equal to W_c, then the model mass decrease is

$\Delta m_0 = (\rho_b - \rho_f) W_c$ in beginning of the path;

$\Delta m_0 = \rho_b W_c$ in the path end.

As a result, the initial impulse is

$$K_1 = [m_0 - (\rho_b - \rho_f)W_c]V_0 . \tag{32}$$

During the propeller work the impulse K_f will be obtained by Eq. (31), and general available impulse will be

$$K_0 = W_c[\rho_f Q_f^{'} - (\rho_b - \rho_f)V_0] .$$

The expression in brackets vanishes at

$$V_{cr} = Q_f^{'} \frac{\rho_f}{\rho_b - \rho_f} . \tag{33}$$

When $V_0 < V_{cr}$, the initial impulse increases, and we can hope that the range increases. On the contrary, when $V_0 > V_{cr}$, it decreases, and we can wait for the model with propeller passes smaller distance than solid one.

4.2 INFLUENCE OF A MISSILE PROPELLER ON THE MODEL MOTION RANGE

Models h1 – h4 with length 250 mm and with length 150 mm were chosen as base-models to research influence of the missile propeller on the model motion range (Table1).

Table 1

Characteristics of models of a series h

N	L cm	R_n cm	R_e cm	m_o g	m_e g	W_f cm^3	M_f G	Δm %	m_f %
1	2	3	4	5	6	7	8	9	10
h1	25	0.05	0.7	156	115	5.3	98	27	6.3
h2	25	0.15	1.525	749	578	21.0	39	22	5.2
h3	15	0.15	1.225	277	227	6.5	12	18	4.3
h4	15	0.15	1.225	277	218	7.5	14	21	5.0

Note: m_o is the solid model mass; m_e is the mass of model with chamber; W_f is the chamber volume; m_f is the fuel mass.

It was accepted that the chambers having truncated cone shape were made in models to dispose the fuel. A diameter of the frontal base of the chamber was accepted equal to the half-diameter of the model in the place of the chamber base disposition. A diameter of the back base was accepted equal to the half-diameter of the tail part of the model.

As a result, four models were developed. They are designated as models of a series h. These models characteristics are given in Table1. Their schemes are shown in Fig. 14. Models h3 and h4 differs by the chamber dimension only.

The calculations were carried out by using the program CDILM. We varied the starting velocity of the model (1200, 1000, 800 and 600 m/s) and specific impulse of the fuel (200, 400 and 600 kg_f /(kg/sec)). The fuel density was accepted equal to 1.85 g/cm^3 in all the cases.

Calculations for the case, when the fuel density was equal to the model material density (7.85 g/cm^3), and its specific thrust was equal to zero, were performed for comparison. This case corresponds to the case of the solid model without propeller.

It is accepted in the calculations that the combustion occurs at constant velocity. All the fuel had burnt during the motion and the fuel combustion continued 1/2 sec to 1/12 sec.

Thus, the model was passing the greatest part of the path at the operating propeller.

One can see changing the model material on the fuel does not give an gain in the range for any model at specific impulse Q_f = 200. The most effective fuel gives some gain in the range from 30% at high starting velocity to 150 % at low one (Fig. 15).

5. Interaction between the propeller and supercavity

Problems on interaction between the propeller and a supercavity are weakly studied direction of the hydrodynamics and enough complex for theoretical and experimental investigation.

The similar problem on interaction between the propeller and ship is known in shipbuilding [16]. This interaction may be both positive:

– the system efficiency increasing at creation of the additional thrust on the hull by means of the pressure redistribution and negative;

– the entraining force increase on the hull and the interaction efficiency reduction of the system "hull-propeller" in dependence on construction of the propeller and hull, their mutual disposition and the propeller work regime.

In this case the propeller can influence on the cavity shape directly by changing its closure conditions, free surface structure and gas-leakage from the supercavity at its presence on the hull.

The following types should be noted among the constructive features of the propellers:

1. Gas jet.

1.1. Jet with condensable phase.

2. Water jet.

3. Screw.

3.1. Supercavitating screw.

4. Turboprop.

The following configurations are noted among the configurations of propellers about the supercavity:

1. The frontal disposition of the propeller or the

towing propeller located in the nose in front of the supercavity.

2. Tail disposition of the propeller or the pushing propeller past the supercavity.

5.1. DESCRIPTION OF PARAMETERS GOVERNING THE DYNAMICS OF CAVITY ENTRAINMENT

The supercavity as the flow form created by free streamlines is very sensitive to the external pressure fields, including the pressure fields formed by the propeller.

As is known from the hydromechanics [16], the propellers always forms jets of gas or fluid modeled by distributed sources and dipoles.

The scheme with ideal propeller [16] (Fig. 16) gives a typical picture of change of the flow parameters. In this case the additional fluid is not injected compared to the case of the jet (Fig. 16), and the working section of the propeller may e modeled by a surface of dipoles oriented so that they pumps the fluid from the zone in front of the propeller to the zone past the propeller. Thus, the pressure difference from $-\Delta P$ to $+\Delta P$ is created in the working section.

It is clear that in the case of interaction with the supercavity the frontal zone with reduced pressure $-\Delta P$ will entrain the cavity, and the cavity will be displaced from the zone with increased pressure $+\Delta P$. It is necessary to consider their joint influence in the real case when the flow is formed both by the hull and the propeller.

Since the propeller must only compensate the impulse loss caused by the hydrodynamic drag of the hull in the free stream, then main dimensionless criterion influencing on behavior of the flow around the propeller with taking the hull into account

$$\overline{T} = \frac{T}{R}, \tag{34}$$

where T is the propeller thrust, R is the hull drag. In this case it is necessary to distinguish three regimes.

When $\overline{T} > 1$, it is the acceleration regime. The thrust is higher than the hydrodynamic drag (the wake past the body has the positive impulse);

When $\overline{T} = 1$, it is the steady motion regime (the wake without impulse);

When $\overline{T} < 1$, it is the deceleration regime(the wake past the body has the negative impulse).

This criterion $\overline{T}$ is the most considerable, because the main consumption of the impulse and energy is included in the propeller thrust. This results in the basic change in the environmental fluid.

It is necessary together with this (34) to take into account the local flow parameters caused by propeller directly in the cavity closure zone.

5.2. CAVITY CLOSURE IN THE GAS JET ZONE OF THE PROPELLER

- **The gas jet is source of gas-supply into the supercavity**

At certain conditions of gas jet outflow, when the jet outflow velocity $\overline{V}_j$ is lower than the critical velocity $\overline{V}_{jCR}$

$$\overline{V}_j = \frac{V_j}{V_\infty} < \overline{V}_{jCR}, \tag{35}$$

the gas part may return from the jet boundary layer into the cavity and be the additional gas-supply.

- **The gas jet is the ejector (sink) sucking out the gas from the cavity**

This regime may be observed when $\overline{V}_j$ exceeds the critical velocity $\overline{V}_{jCR}$

$$\overline{V}_j = \frac{V_j}{V_\infty} > \overline{V}_{jCR}, \tag{36}$$

The criterion $\overline{V}_{jCR}$ depends on the place and conditions of the cavity closure. So the criterion $\overline{V}_j$ (35), (36) is the second parameter governing the dynamics of supercavity.

5.3. INTERACTION BETWEEN THE CAVITY AND PROPELLER. TAIL LOCATION OF THE PROPELLER

Experiments on study of the propeller influence on the cavity were carried out at the IHM on the special installation (Figs. 17, 18). On this installation the supercavity was formed by means of the ring cavitator on the hull with diameter D_m = 52 mm which is in front of the propeller with blades.

Pictures of flow around the model at different regimes of the propeller work at continuous gas-supply are shown in photos (Figs. 19, 20, 21).

5.4. FRONTAL LOCATION OF THE SCREW PROPELLER

Investigation of the propeller screw influence on the cavity was carried out on the special installation permitting to create the artificial cavity around the propeller tail cone at different regimes of the propeller screw work. A ratio of the screw and cavity diameter was $D_p = (2 \div 3)D_m$. The propeller screw is located in the nose part in front of the cavity. It is established in virtue of the fulfilled researches that the working propeller screw considerably changes the cavitation characteristics of the tail cone [15].

Results of the cavity testing for the working propeller screw are given in the form of dependencies of the relative parameters of the artificial cavity as function of the screw load coefficient $K_p = \frac{8K_1}{\pi\lambda_p^2}$, where K_1 is the thrust coefficient, and λ_p is the relative screw tread.

Changes of the cavity length $\overline{L} = \overline{L}_p / L_0$, cavitation number $\overline{\sigma} = \sigma_p / \sigma_0$ and air rate coefficient $\overline{Q} = Q_p / Q_0$, where L_0, σ and Q_0 are the isolated cavity parameters at absence of the propeller screws but at other the same conditions, are given in Figs. 22, 23, 24, respectively. As is shown in the graphs, the cavity length considerably decreases when the propeller screw is located in front of the cavity. It is about 30% of the isolated cavity length even at zero load of the screw and the same air rate. In this case the cavitation number increases but considerably slower than the cavity length changes. This is explained to that the propeller screw not only increases the pressure downstream and strongly swirls the stream. As a result, the cavity boundary is destroyed. To reach the same cavity length at the working propeller screw it is necessary to increase in some times the air rate. So, when $K_p = 0$, the consumable air rate must exceed in 2-3 times the corresponding value of Q_0 for the isolated cavity, and when $K_p = 0.3$, it is necessary to increase in 5 times the air rate (Fig. 24).

References

1. Epshtein L.A. Methods of theory of dimensionality and Similarity for problems of Ship Hydromechanics. –Leningrad, Sudostroenie, 1970, 207 p., (in Russian).
2. Gurevich M.I. Theory of jets of ideal fluid. – New-York – London, Academic Press, 1965.
3. Problems and methods of hydrodynamics of underwater foils and screws. – Kiev, Naukova dumka, 1966. – 160 p., (in Russian).
4. J. Nielsen. Missile aerodynamics. Mc. GRAW-HILL BOOK COMPANY, New York, Toronto, London, 1960. 474 c.
5. Borisyuk M.N. Problem on vertical hydrofoil. // J. Hydrodynamics of High Speeds. – Kiev, Naukova dumka, 1966. P. 59 - 74, (in Russian).
6. Pantov Ye.N., Mahin N.N., Sheremetov B.B. Foundations of theory of motion of underwater vehicles. Leningrad, Sudostroenie, 1973. – 211p., (in Russian).
7. Cascade wings. At edition of Belotserkovsky S.M. – Moscow, Mashinostroenie, 1985.-390 p., (in Russian).
8. Belotserkovsky S.M., Nisht M.N. Separated and continuous flow around slender wings in ideal fluid. – Moscow, Nauka, 1978. – 351 p., (in Russian).
9. Underwater projectile. Franklin A. Monson. US patent 3.915.092, 10.28.1975.
10. Logvinovich G.V. Hydrodynamics of flows with free boundaries. Kiev, Naukova dumka, 1969. – 208 p., (in Russian).
11. Savchenko Yu.N. Investigation of High-Speed Supercavitating Underwater Motion of Bodies. AGARD Report 827 "High Speed Body Motion in Water", 1998, FDP Wokrshop, Kiev. – P. 20-1 – 20-12.
12. Savchenko V.T. Reduction of overload on a body entering in water at high speed. AGARD Report 827, High Speed Body Motion in Water. Kiev, 1997. – P. 29-1 – 29-6.
13. Savchenko Yu. N., Putilin S.I., Savchenko V.T. Aerohydrofoil. Patent USSR, Inform Bull. 5, 1992.
14. Savchenko V.T. Hydrodynamic Characteristics of Rudders Operating in Air-Sea Interface. RTO AVT Symposium Papers "Fluid Dynamics Problems of Vehicles Operating near or in the Air-Sea Interface", Amsterdam, 1998. P. 17- 1 – 17-9.
15. Yegorov I.T. Artificial cavitation. – Leningrad, Sudostroenie, 1971, 283 p.
16. Voytkunski Ya.I. Handbook on ship theory. – Leningrad, Sudostroenie, 1960.
17. L.M. Milne-Tomson, C.B.E. Theoretical hydromechanics. – London, Macmillan & CO LTD, 1962.
18. Migirenko G.S. and others. Some ways of cavity flow control at low Froude numbers. Proc. of Symp. IUTAM.- Moscow, Nauka, 1973, p. 361 – 367.
19. Leonard Greiner. Underwater Missile Propulsion. – 1967. Compas Publ. Inc., VA, USA.
20. Putilin S.I. Some peculiarities of dynamics of supercavitating models. // J. of Applied mechanics. Vol. 2, No 3, 2000, pp. 65 – 74.
21. Ivchenko V.I., Grigoriev V.A., Prihodko N.A. Optimal hydroreactive systems. Krasnoyarsk Univ., 1985.
22. Savchenko Yu.N. Perspective of hydrodynamic drag reduction methods. // J. of Applied mechanics. Vol. 1, No 4, 1999, pp. 42 – 50.
23. Semenenko V.N. Dynamics of supercavitating bodies. Symp. on High-Speed Hydromechanics and Supercavitation.March 31, 2000, Grenoble, France, pp. 1 – 15.

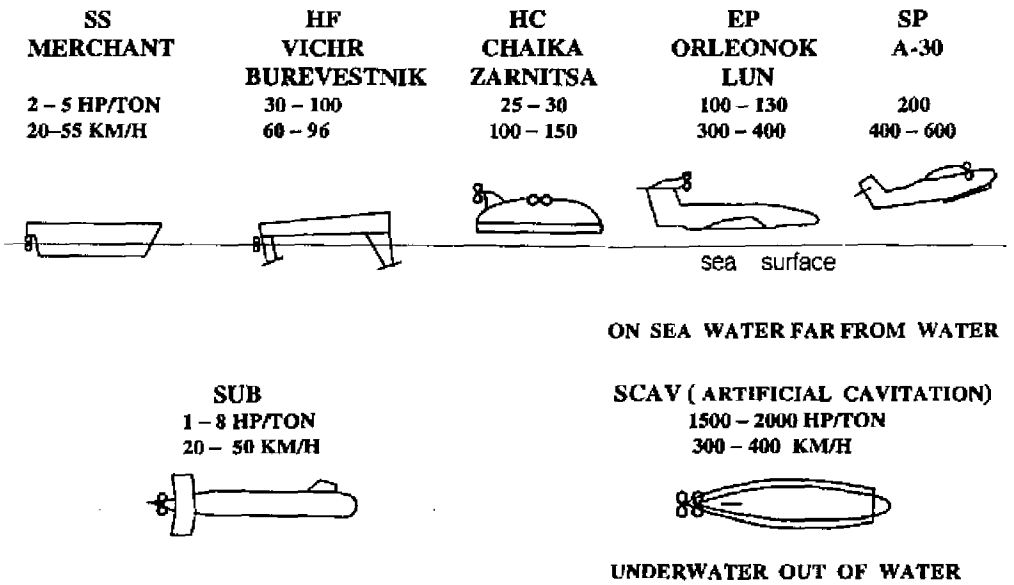
SS
MERCHANT
2 – 5 HP/TON
20–55 KM/H
HF
VICHR
BUREVESTNIK
30 – 100
60 – 96
HC
CHAIKA
ZARNITSA
25 – 30
100 – 150
EP
ORLEONOK
LUN
100 – 130
300 – 400
SP
A-30
200
400 – 600
sea surface
ON SEA WATER FAR FROM WATER
SUB
1 – 8 HP/TON
20 – 50 KM/H
SCAV (ARTIFICIAL CAVITATION)
1500 – 2000 HP/TON
300 – 400 KM/H
UNDERWATER OUT OF WATER

Fig. 1

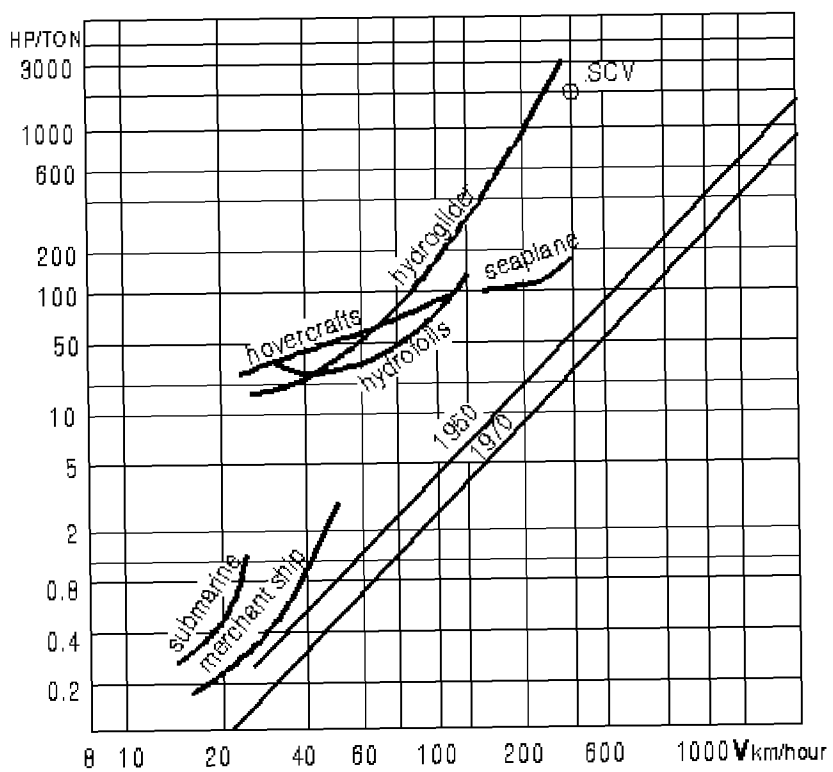
HP/TON
3000
1000
600
200
100
50
10
5
2
0.8
0.4
0.2
SCV
hydrogliter
seaplane
hovercrafts
hydrofoils
1950
1970
submarine
merchant ship
8
10
20
40
60
100
200
600
1000
V km/hour

Fig. 2

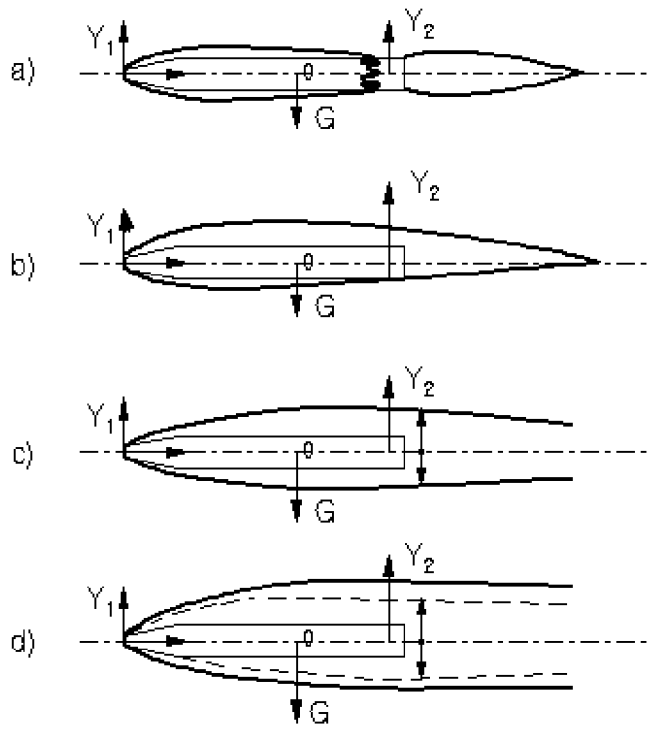
a)
b)
c)
d)
Y_1
Y_2
G

Fig. 3

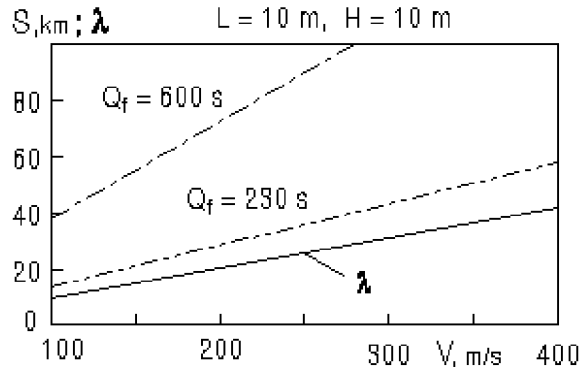
S,km; λ
L = 10 m, H = 10 m
Q_f = 600 s
Q_f = 250 s
λ
80
60
40
20
0
100
200
300
V, m/s
400

Fig. 4

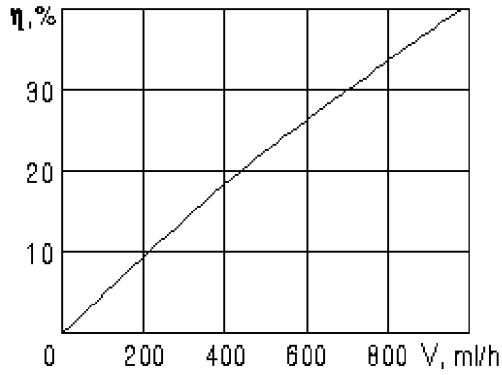
η, %
30
20
10
0
200
400
600
800
V, ml/h

Fig. 5

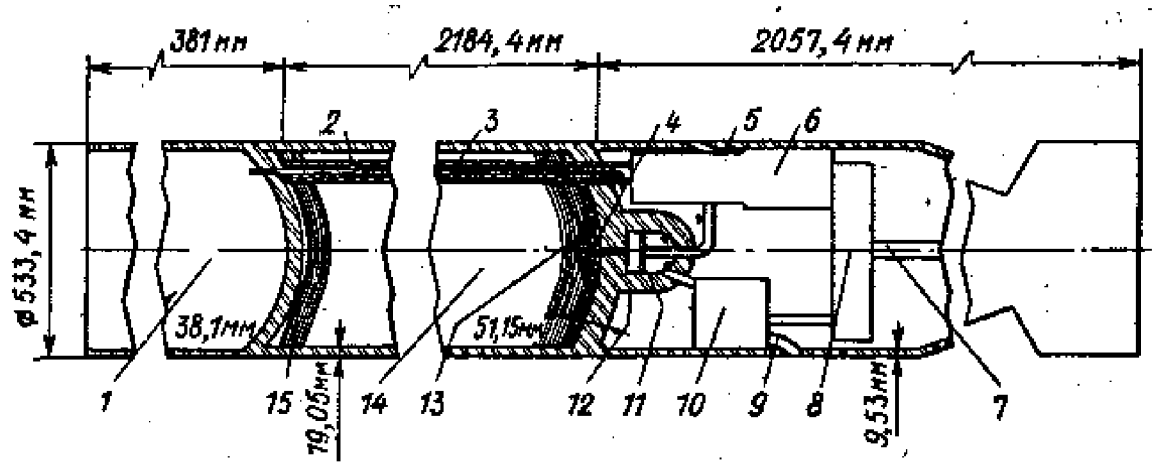
381 мм
2184,4 мм
2057,4 мм
ф 533,4 мм
38,1мм
51,15мм
19,05мм
9,53мм
1
2
3
4
5
6
7
8
9
10
11
12
13
14
15

Fig. 6b

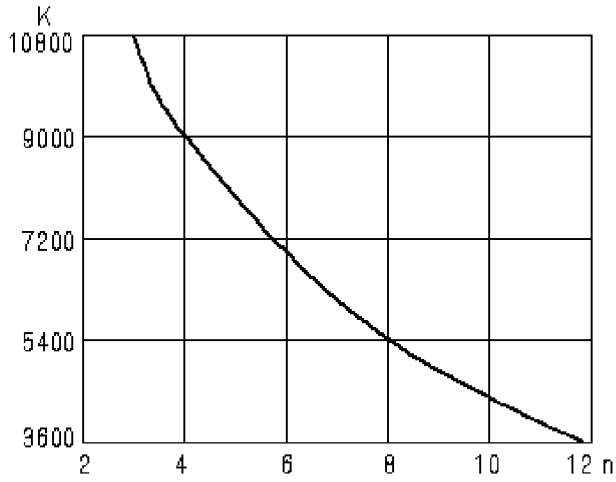
K
10800
9000
7200
5400
3600
2
4
6
8
10
12 n

Fig. 6a

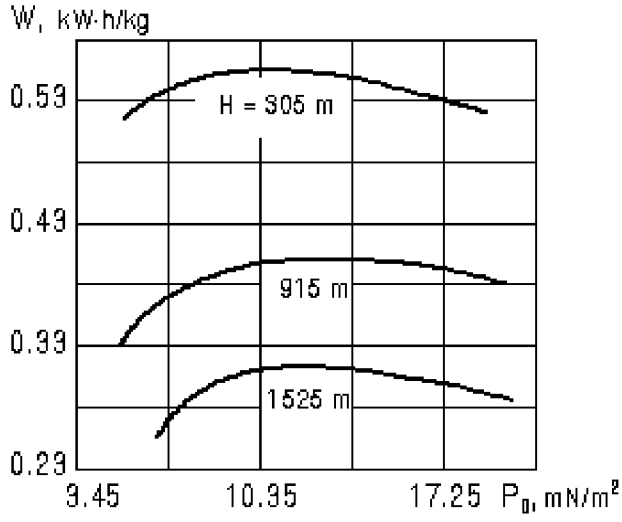
W, kW·h/kg
0.53
0.43
0.33
0.23
H = 305 m
915 m
1525 m
9.45
10.35
17.25
P0, mN/m²

Fig. 7

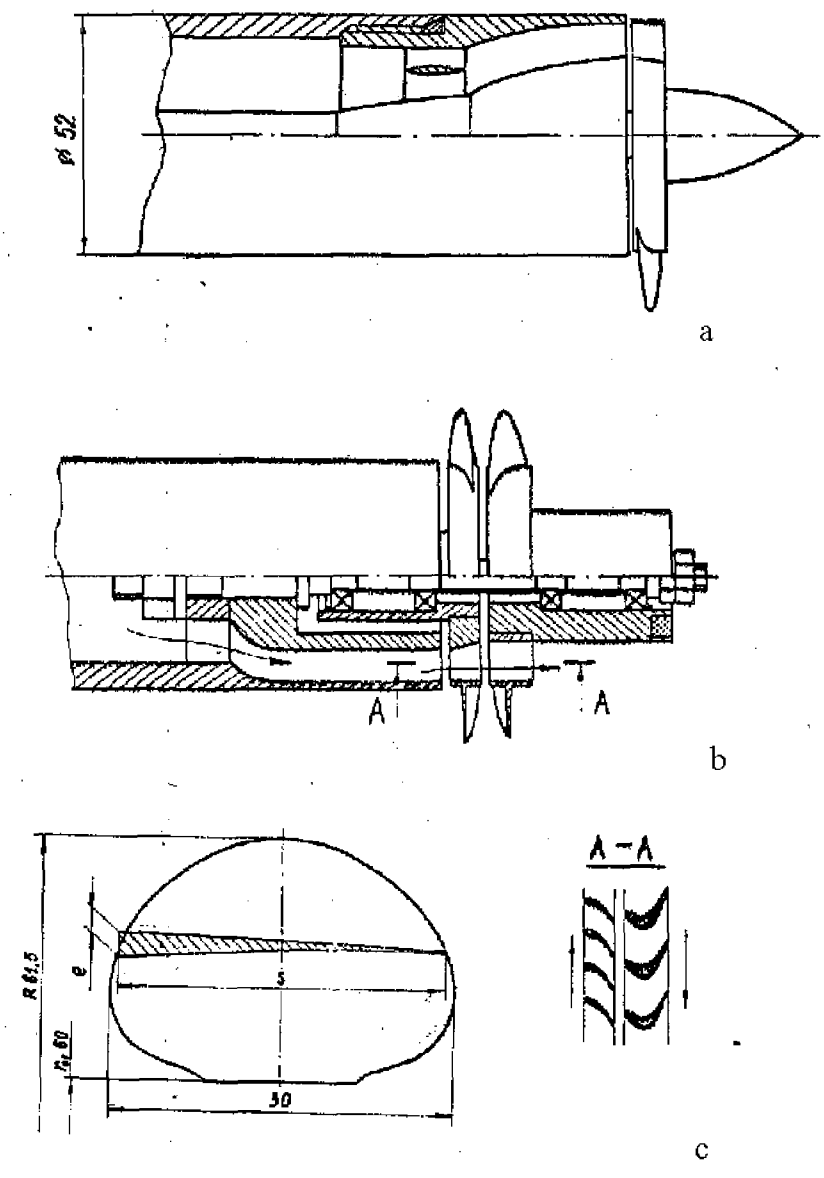

Fig. 8

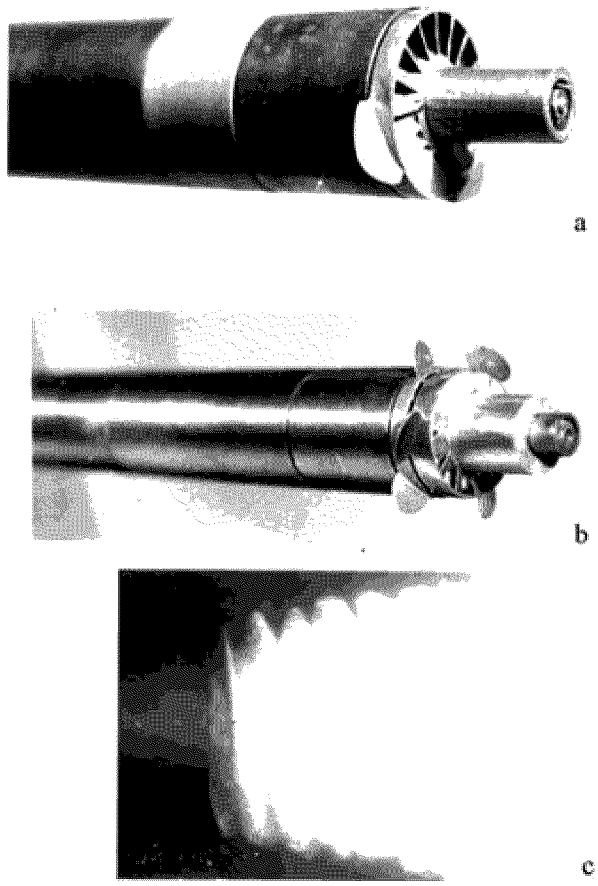

Fig. 9

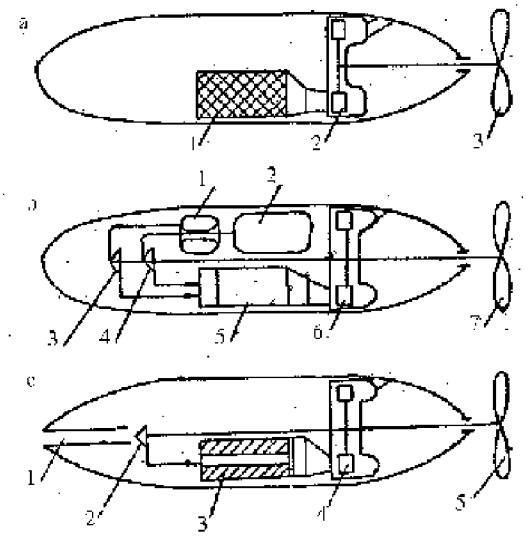

Fig. 10

Properties of different types of the fuel

Fuel	Chemical Formula	Density, g/cm3	Molecular weight	Temperature of melting	Temperature of boiling	Reaction	Molecular weight of reaction product	Quantity of evolved hydrogen , l/g,	Specific heat of reaction, Kcal/l	Theoretical velocity of flowing out, m/s	Theoretical specific impulse
Aluminum	Al	2.7	26.98	658	2500	$2Al + 1.5O_2 = Al_2O_3$	101.94	–	3730	5590	570
Aluminum	Al	2.7	26.98	658	2500	$Al + 3H_2O = Al(OH)_3 + 1.5H_2$	81.03	1.25	4150	5900	601
Magnesium	Mg	1.74	24.32	657	1102	$Mg + 0.5O_2 = MgO$	40.32	–	3623	5510	562
Magnesium	Mg	1.74	24.32	657	1102	$Mg + 2H_2O = Mg(OH)_2 + H_2$	60.32	0.924	3800	5640	575
Lithium	Li	0.534	6.94	179	1372	$2Li + 2H_2O = 2LiOH + H_2$	49.88	1.62	5340	6700	683

Fig. 11

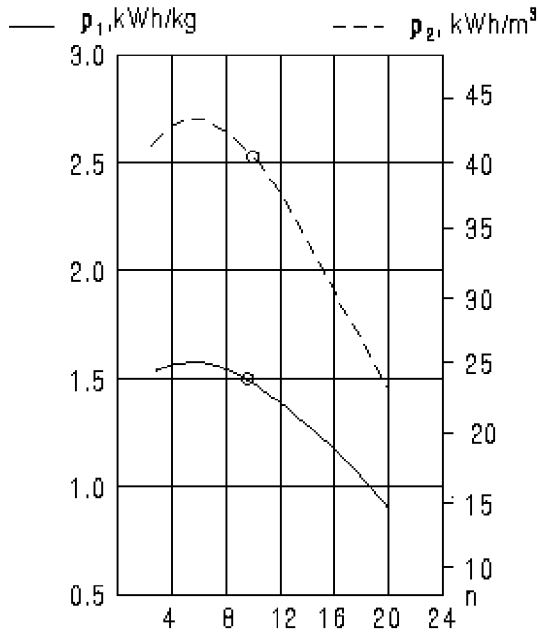

Fig. 12

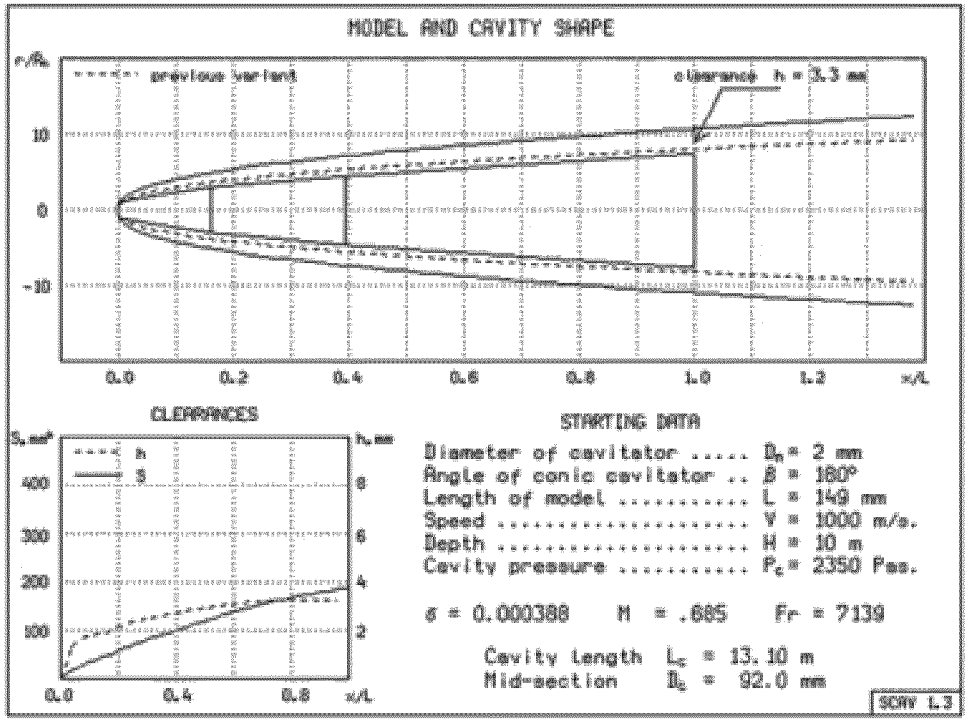

Fig. 13a

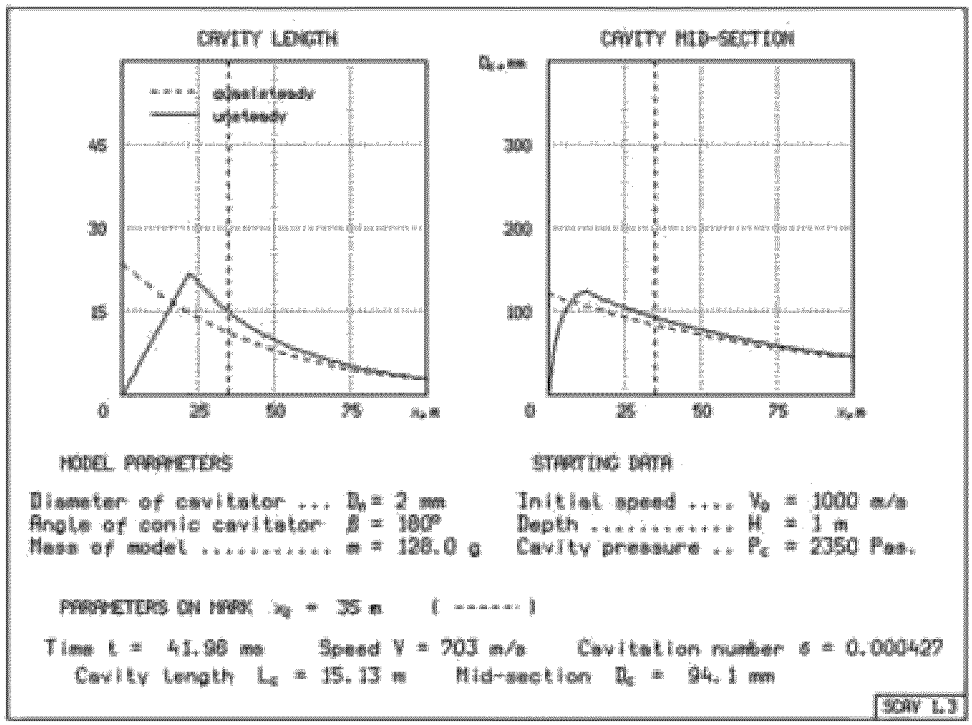

Fig. 13b

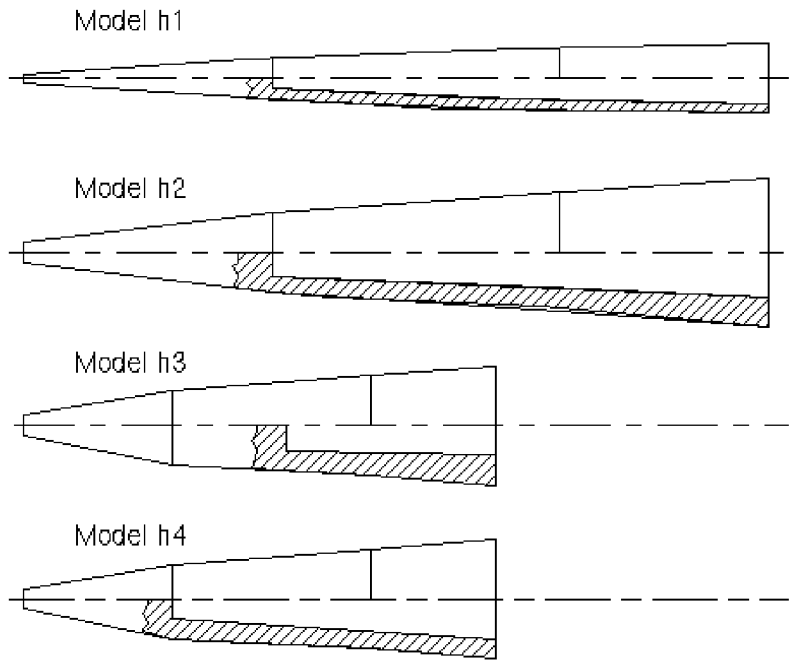
Model h1
Model h2
Model h3
Model h4

Fig. 14

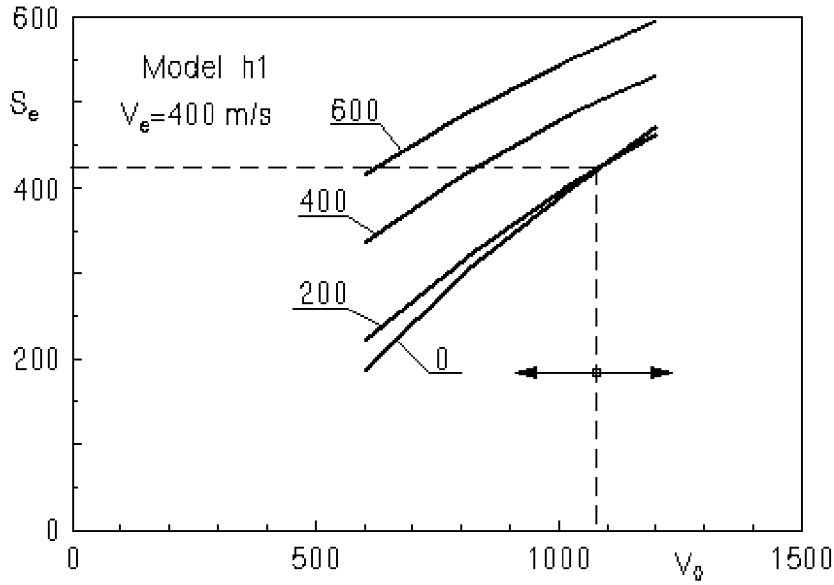
600
400
200
0
S_e
Model h1
V_e=400 m/s
600
400
200
0
0
500
1000
1500
V_0

Fig. 15

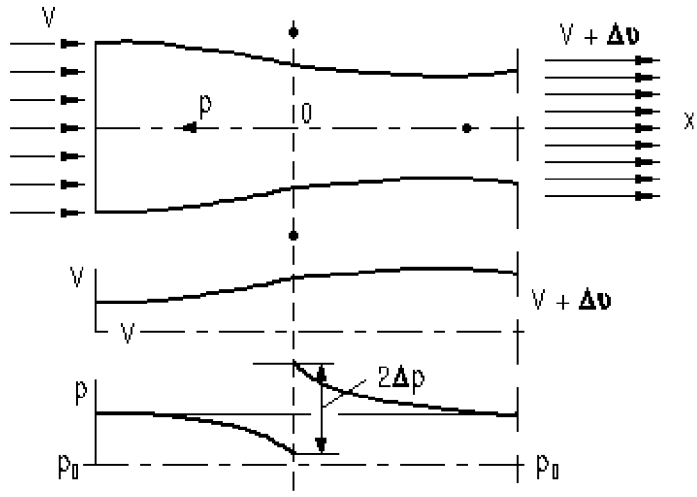

Fig. 16

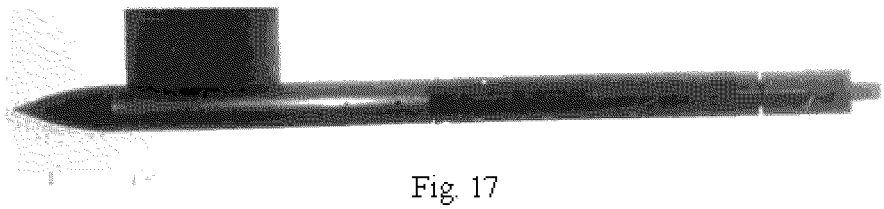

Fig. 17

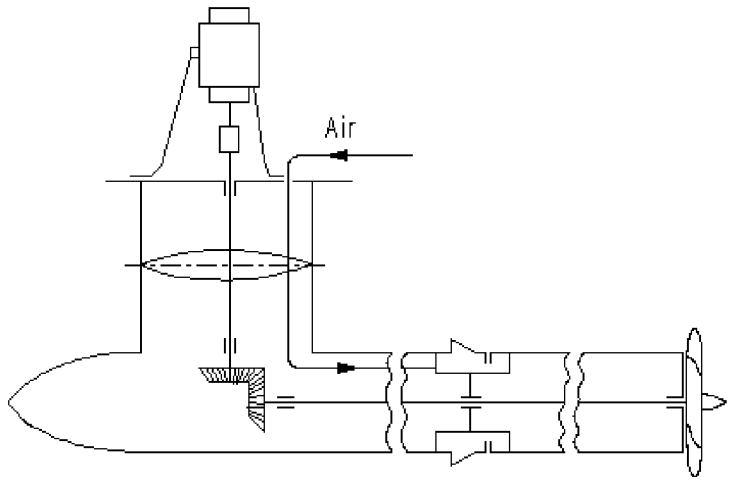

Fig. 18

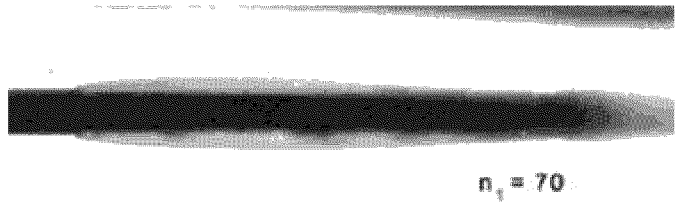

Fig. 19

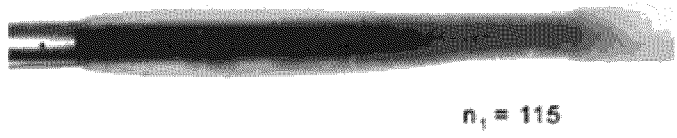

Fig. 20

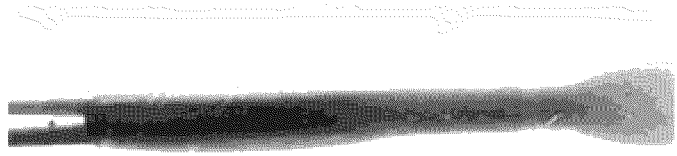

Fig. 21

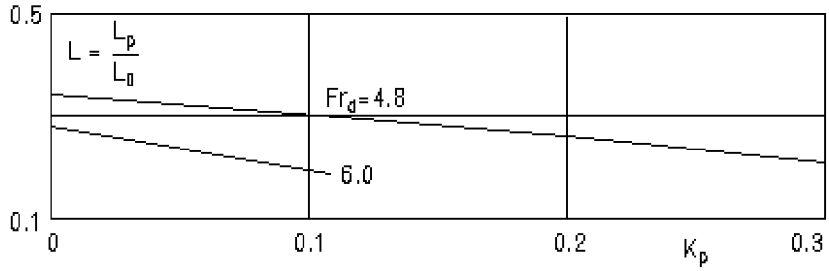

Fig. 22

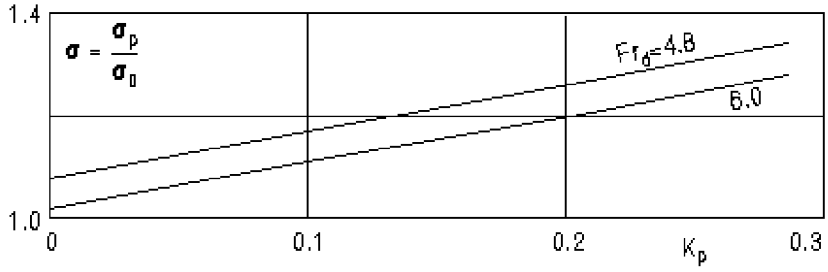
1.4
1.0
$\sigma = \frac{\sigma_p}{\sigma_0}$
Fr_d=4.8
6.0
0
0.1
0.2
K_p
0.3

Fig. 23

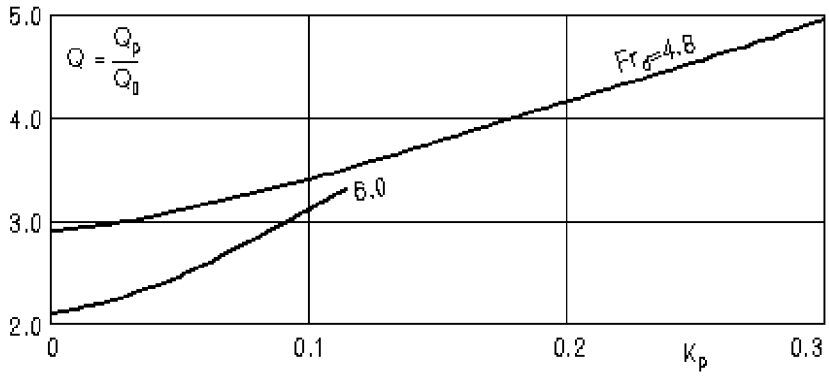
5.0
4.0
3.0
2.0
$Q = \frac{Q_p}{Q_0}$
Fr_d=4.8
6.0
0
0.1
0.2
K_p
0.3

Fig. 24